

Supplemental Material

Impaired renal reserve contributes to preeclampsia via the kynurenine and soluble fms-like tyrosine kinase 1 pathway

Vincent Dupont^{1,2}, Anders H. Berg³, Michifumi Yamashita³, Chengqun Huang³, Ambart E. Covarrubias¹, Shafat Ali¹, Aleksandr Stotland⁴, Jennifer E. Van Eyk⁴, Belinda Jim⁵, Ravi Thadhani⁶, and S. Ananth Karumanchi¹

¹Department of Medicine, Cedars-Sinai Medical Center, Los Angeles, CA

²EA-3801, Université de Reims Champagne-Ardenne, Reims, France

³Department of Pathology and Laboratory Medicine, Cedars-Sinai Medical Center, Los Angeles, CA

⁴Department of Biomedical Sciences and Smit Heart Institute, Cedars-Sinai Medical Center, Los Angeles, CA

⁵Department of Medicine, Jacobi Medical Center, Albert Einstein College of Medicine, Bronx, NY

⁶Department of Medicine, Massachusetts General Hospital, Harvard Medical School, Boston, MA

SUPPLEMENTAL METHODS

Glomerular Filtration Rate (GFR) measurements:

To validate estimated GFR equations in mice, we directly measured GFR, plasma creatinine and cystatin C levels in an independent cohort of mice with varying degrees of renal insufficiency (N=17). Of these 17 mice, 6 animals had ischemia-reperfusion injury (1), 4 animals had uninephrectomy, 2 animals had CKD from oxalate nephropathy (2), 1 animal had CKD from genetic ablation of podocytes (3) and 4 with no kidney disease. Plasma creatinine (Diazyme) and cystatin C (Quantikine ELISA Mouse/Rat Cystatin C Immunoassay, R&D Systems) were measured according to manufacturer's instructions. GFR was measured using a FITC-sinistrin transdermal device (MediBeacon) as described elsewhere (4). Briefly, skin fluorescence was continuously recorded by the device during 1 hour following the retro-orbital injection of 5mg/100g body weight of FITC-sinistrin. Data were extracted and analyzed using MBstudio and MBlab softwares (MediBeacon) to calculate GFR. We then tested different models (linear, polynomial, logarithmic, exponential, power) to assess the best correlation of GFR with plasma creatinine and cystatin C concentrations based on r squared values. The best correlation was found using cystatin C measurements with the linear model (Supplemental Figure 1 C-D). In all subsequent experiments, we evaluated renal function by measuring cystatin C levels by ELISA and calculating estimated GFR (eGFR) values using the following formula: $GFR \text{ (mL/min/100g body weight)} = -3.2886 * \text{plasma cystatin C } (\mu\text{g/mL}) + 2.9409$.

Quantification of L-kynurenine pathway metabolites

Measurements of L-kynurenine and metabolites of L-kynurenine were performed using high performance liquid chromatography and isotope-dilutional mass spectrometry. All non-isotopic chemicals, except when noted, were purchased from Sigma-Aldrich, Saint Louis, MO; all isotopic standards, except when noted, were purchased from Toronto Research Chemicals, Toronto, Canada. Briefly, 10 microliters of plasma were mixed with 10 microliters of a 50 micromole/L mixture of isotopic standards diluted in water (L-kynurenine-d₄, Quinolinic acid-¹³C₃,¹⁵N₁, Nicotinic acid riboside-d₄, NAD⁺-d₅, L-tryptophan-d₅ (CDN Isotopes, Pointe-Claire, Canada), nicotinamide-¹³C₆ (Sigma Aldrich, St. Louis, MO)). Plasma proteins were then precipitated by mixing with 80 µL acetonitrile (80% final conc.), and precipitates were cleared by centrifuging at 14,000 rpm for 10 minutes. Supernatant was transferred into a 96-well plate for analysis. Analysis was performed using an API 5500 triple quadrupole mass spectrometer from AB Sciex (Foster City, CA) coupled to a Shimadzu Prominence UFLC liquid chromatography system with autosampler (Shimadzu Scientific Instruments, Columbia, MD). High performance reverse phase chromatography was performed by injecting 15 microliters of plasma supernatant onto a Kinetex Polar C18 UPLC column (150 x 4.6 mm, 2.6 µm bead diameter, 100A pore size, Phenomenex, Inc., Torrance, CA) using a gradient elution protocol detailed in Supplemental Table S2. MS/MS transitions and settings for multiple reaction monitoring (MRM) of each metabolite is shown in Supplemental Table S3. Instrument control, data acquisition and quantification were performed using Analyst 1.6.2 software (Sciex, Framingham, MA). Calibration standards for each metabolite (L-tryptophan, L-kynurenine, quinolinic acid, kynurenic acid, nicotinamide, nicotinic acid,

NAD⁺, nicotinamide mononucleotide, and indoxyl sulfate) were diluted into phosphate buffered saline, standard curves for each metabolite were generated by running calibrator mixtures at 0, 12.5, 25, 50, and 100 micromoles/L for each metabolite. L-kynurenine-d4 was used as the internal standard for kynurenic acid and nicotinamide mononucleotide, quinolinic acid was used as internal standard for indoxyl sulfate. NAD⁺-d5 was internal standard for NAD⁺ and NADH measurements. Metabolite concentrations were measured by quantifying the area under the curve (AUC) for each MRM transition and normalizing it to its respective isotopic standard and metabolite/internal standard ratio was converted into absolute concentrations according to each standard curve.

SUPPLEMENTAL REFERENCES

1. Poyan Mehr A, Tran MT, Ralto KM, Leaf DE, Washco V, Messmer J, et al. De novo NAD(+) biosynthetic impairment in acute kidney injury in humans. *Nat Med*. 2018;24(9):1351-9.
2. Luz HL, Reichel M, Unwin RJ, Mutig K, Najenson AC, Tonner LM, et al. P2X7 Receptor Stimulation Is Not Required for Oxalate Crystal-Induced Kidney Injury. *Sci Rep*. 2019;9(1):20086.
3. Stotter BR, Talbot BE, Capen DE, Artelt N, Zeng J, Matsumoto Y, et al. Cosmc-dependent mucin-type O-linked glycosylation is essential for podocyte function. *Am J Physiol Renal Physiol*. 2020;318(2):F518-F30.
4. Scarfe L, Schock-Kusch D, Ressel L, Friedemann J, Shulhevich Y, Murray P, et al. Transdermal Measurement of Glomerular Filtration Rate in Mice. *J Vis Exp*. 2018(140).

SUPPLEMENTARY TABLES

Table S1: Raw data for Metabolomic profiling in non-pregnant state and during pregnancy in uninephrectomized mice and controls

Table S2. HPLC setting for Reverse Phase Chromatography

Table S3: MRM Mass Spectrometer Settings for isotope dilutional quantification of metabolites

Orotic acid	10.6353778	28.2228823	26.0009066	11.4580975	65.6114936	12.8707679	20.3633996	29.6142525	35.5263333	0.7810596	11.8872492	13.8545222	13.9348746	15.5740418	11.8097276	21.8060423
O-Succinyl-L-homoserine	0.72650466	9.29822502	0.33186934	1.51483231	1.78582053	1.25886354	0.07410025	0.87607454	2.5320654	6.39304035	2.33862174	0.96489116	4.6142085	1.79118841	1.17381181	0.18822279
Oxamic acid	0.263739281	0.019388248	0.102343217	0.021629235	0.127028632	0.070912255	0.014196147	0.048795168	0.35723472	0.12507275	3.795140181	0.045419741	0.18183078	0.076826558	0.045923984	0.007348051
Phenylpyruvic acid	85.53338	37.67909	68.29974	74.12495	16.26408	31.69179	64.87049	33.28819	297.19949	61.83541	120.98398	43.5151	11.65828	26.68131	22.62059	56.9879
Phosphoenolpyruvic acid	1.6303856	1.2381117	0.2964832	2.370477	5.7914277	0.7591647	10.2619166	1.2319255	0.308313	0.6251913	0.5571945	0.9208046	3.3803241	10.9433398	0.3716569	1.6592452
Prephenic acid	0.68927645	0.31479773	0.447855	0.90008314	0.20831101	0.7070545	1.02358855	0.504322	1.33883388	0.75553035	0.41190262	0.30987006	0.08056539	0.60823444	0.17655564	0.02901105
Pyridoxal 5 phosphate	0.075336759	0.017127015	0.01110873	0.014943375	0.050115883	0.022589205	0.046626203	0.055704192	0.021255068	0.018719933	0.089694486	0.035136016	0.006347538	0.029838638	0.013700744	0.026967082
Pyridoxal hydrochloride	42.971801	22.932938	33.784443	47.40208	17.408739	14.244428	24.452615	41.440032	33.862064	20.42786	31.767489	20.983786	8.180867	8.159778	7.673163	12.723306
Pyridoxamine	0.11679365	0.04288198	0.01456488	0.0218282	0.03771099	0.04293612	0.1148956	0.02387835	0.14657243	0.08577451	0.04930666	0.01536083	0.01852693	0.06617169	0.02127728	0.01064408
Pyridoxine	0.044493597	0.007196009	0.006295666	0.023729212	0.070349787	0.019431254	0.042401331	0.036549522	0.056198589	0.025989017	0.004748002	0.023223903	0.033031548	0.006200268	0.027843976	0.018959462
Pyruvic acid	35.02923	27.875	19.36074	18.29951	40.46649	23.4249	80.03653	41.41164	36.17542	10.89089	34.39794	15.39854	14.66961	22.15831	26.99408	62.41118
Quinic acid	0.13778051	0.18000788	37.16565924	0.38161654	0.97052181	0.41578876	0.54156989	28.33782229	0.32763342	0.1548903	0.06937234	1.49746128	0.24567657	0.10987652	2.19237885	0.49173379
Riboflavin	4.515492	2.785324	3.313833	4.71573	12.306436	6.155485	11.413775	9.051999	6.661967	4.589127	5.671828	2.663282	4.73074	5.082106	4.419727	9.686734
Ribonic acid gamma lactone	0.20691163	0.23131798	0.2348918	0.13086506	0.15514418	0.30344788	0.42818377	1.43016818	0.13928131	1	0.12720405	0.2009589	0.03274399	0.41875554	0.07986553	0.1099699
S-2-Aminoethyl-L-cysteine	0.002901588	0.00923276	0.022540821	0.003613196	0.00577006	0.027189538	0.010029739	0.073024269	0.005042682	0.067568963	0.006095564	0.002396469	0.001504584	0.019494938	0.003383335	0.0021842
S-5-Adenosyl-L-homocysteine	0.19894066	2.0686985	0.02615313	0.07931886	0.54488491	0.05262932	0.06323973	0.69695247	0.05439666	0.21629759	0.20392384	0.04033733	0.0729446	0.2750385	0.01637844	0.04953528
Salicylic acid	329.8524	310.4768	483.8678	766.9512	833.9231	466.9752	1069.2726	1029.118	1287.4672	227.151	415.0164	281.2373	597.7789	961.1854	621.6994	927.7229
Shikimic acid	0.03113439	0.08934497	0.21284233	0.07301461	0.04906816	0.01708142	0.02615886	0.08620594	0.07827334	0.02780046	0.06830827	0.077785	0.01240901	0.06609093	0.02850468	0.06150173
Succinic acid	1179.095	1238.372	1379.813	1512.976	3196.488	2037.588	4982.965	2879.364	6130.856	2281.244	3492.275	1565.839	1876.563	1815.952	2101.673	6417.874
Succinic semialdehyde	0.3438837	0.30598756	0.27655161	0.18199817	0.14300014	0.70279983	0.17117968	0.53032019	0.59531827	0.73101034	0.04037461	0.34842622	0.01776637	0.13568803	0.04517473	0.0960843
Taurine	194.43822	84.90006	183.90929	199.56113	326.55769	190.33069	248.28945	361.59651	204.97762	287.77536	195.7684	93.20726	256.43602	217.48428	195.67688	377.40196
Taurolcholic acid	20.01509	52.74035	77.07931	63.96632	44.03781	140.4937	192.39049	67.90539	204.77907	173.61252	249.18632	97.38499	156.94134	82.85692	261.79531	53.25747
Thiamine	1.12720448	0.09299369	0.08005223	0.08784045	1.16479442	0.28651631	0.88074909	0.34875937	0.34123027	0.11856902	0.28938846	0.13480289	0.12310614	0.3848235	0.31782153	0.22388268
Thymidine 5-diphosphate	0.077730288	0.007209742	0.061177445	0.035654943	0.070996636	0.156383312	0.123939315	0.075204973	0.122574033	0.100632316	0.175013395	0.022047304	0.013167042	0.073332296	0.01335423	0.153045699
Thymidine	25.4837	38.93717	20.63798	25.54321	45.89581	53.25092	53.36397	25.12125	68.50346	24.58422	20.19781	17.7291	11.75378	15.38223	12.82308	22.64527
Thymine	0.33192706	0.69114871	0.65941921	0.09935941	4.07702254	3.64862268	4.53930121	3.18406507	2.95812046	1.99437058	1.99590302	1.16350323	1.44532693	2.12169763	1.00078347	0.97376395
trans-4-Hydroxy-L-proline	0.06514946	0.07009803	0.09037278	0.04188319	0.23771131	0.25884133	0.34638653	0.22433999	0.07759717	0.0626705	0.04229308	0.0326186	0.07351541	0.03848751	0.13488306	0.1068863
trans-Aconitic acid	523.1912	682.5211	1453.1724	1005.5091	2891.6146	776.654	2318.7474	755.0236	4266.8872	1597.0428	1201.7106	880.8064	1747.1306	856.9428	930.1368	1082.3195
trans-trans Muconic acid	0.024343916	0.027215752	0.060941276	0.030727941	0.023928524	0.032240114	0.008382271	0.002059461	0.013340972	0.047688435	0.021664256	0.016039198	0.012392712	0.009409097	0.013335116	0.043476736
Trehalose 6-phosphate	0.10926377	0.12882636	0.0532332	0.0881463	0.02758386	0.07279972	0.08814052	0.07584365	0.01923868	0.01938302	0.07759289	0.04245136	0.03412834	0.01730092	0.09963334	0.13674588
Trehalose	0.8553901	0.5101067	0.780271	0.635022	0.5168707	0.7146772	0.6576389	0.2199471	1.0660047	1.2227082	0.551616	0.4046044	0.1924801	0.192104	0.3114386	0.2722653
Uracil	33.063274	5.174642	24.49343	1.261119	81.806346	100.812019	250.408164	78.382217	55.722572	56.288331	36.14182	21.825906	33.832382	43.90002	59.739791	158.417795
Uric acid	6321.8697	4582.5309	6103.8525	877.2656	5423.8641	672.6707	3254.5835	1910.9265	139.2098	1087.6152	1032.8977	5035.8736	3109.9306	1805.2304	994.5981	2357.2436
Uridine 5'-diphosphogalactose	17.6581199	14.1906053	15.1433512	15.8676524	7.2073714	13.6960212	5.0097214	0.7709553	23.123437	6.085056	0.6316033	6.6292227	8.4997606	31.2383713	2.23123	5.0486764
Uridine 5-diphosphate	0.05973995	0.073929444	0.01076934	0.184765898	0.02649034	0.053931604	0.013997341	0.011158899	0.059256201	0.05705908	0.013859659	0.007663177	0.021509888	0.042050608	0.00811383	0.00962856
Uridine 5-diphosphoglucose	17.6581199	14.1906053	15.1433512	15.8676524	7.2073714	13.6960212	5.0097214	0.7709553	23.123437	6.085056	0.6316033	6.6292227	8.4997606	31.2383713	2.23123	5.0486764
Uridine 5-monophosphate	5.71430312	0.7034941	0.97258615	2.3946915	1.01928498	0.80388592	0.02400367	0.58089886	0.7510917	0.22853267	0.65631528	2.45276198	1.65497609	3.89671466	1.21326686	0.19110169
Uridine 5-triphosphate	0.049077733	0.019134367	0.051241206	0.050446256	0.016805628	0.014000282	0.036116294	0.03321787	0.021153138	0.021533729	0.034296311	0.016052333	0.003480788	0.015033264	0.015975416	0.04418328
Uridine	324.9264	69.36707	243.38638	155.19493	110.40218	295.16479	236.04111	105.18128	222.09031	84.45513	91.07905	179.25362	46.84741	98.85334	83.22474	216.60373
Vanillic acid	1.2727152	0.4931905	0.5794625	0.2502396	0.7629475	0.2198843	0.7832157	0.4071818	2.1388803	0.8314462	0.3888596	0.2185147	0.9793995	0.5842783	0.1573207	1.6390328
Xanthine	7.37E-01	6.98E-02	3.51E+02	2.34E-02	6.91E-03	1.10E-01	1.48E-01	5.10E-02	7.41E-02	1.95E-01	1.71E-02	6.59E+01	6.76E+02	4.32E-02	3.15E-02	2.70E-01
Xanthosine	249.04545	234.74997	270.50046	76.41716	508.85908	30.62075	91.51357	76.70194	153.38873	26.41666	32.13758	485.46687	715.72642	34.56154	33.80501	38.80797
Xylitol	1.0666891	0.656876	0.4677887	0.6477543	2.1958953	1.277244	0.9083101	0.4905191	2.0126279	1.3320049	1.4376948	0.9111761	1.5742927	0.7420066	0.7647662	1.139168

Table S2: HPLC setting for Reverse Phase Chromatography

HPLC settings for reverse phase chromatographic separation of plasma metabolites by gradient elution, confirmatory quantification by isotope dilutional MS. Buffer A comprised of 20 mM ammonium formate and 0.05% formic acid in HPLC grade water; Buffer B comprised of acetonitrile with 0.05% formic acid, flow rate 0.6 ml/min.

Time (min)	% Buffer B
0 – 7.0	3% – 50%
7.0 – 7.4	50% - 100%
7.5 – 7.9	100%
8.0 – 10.0	3%

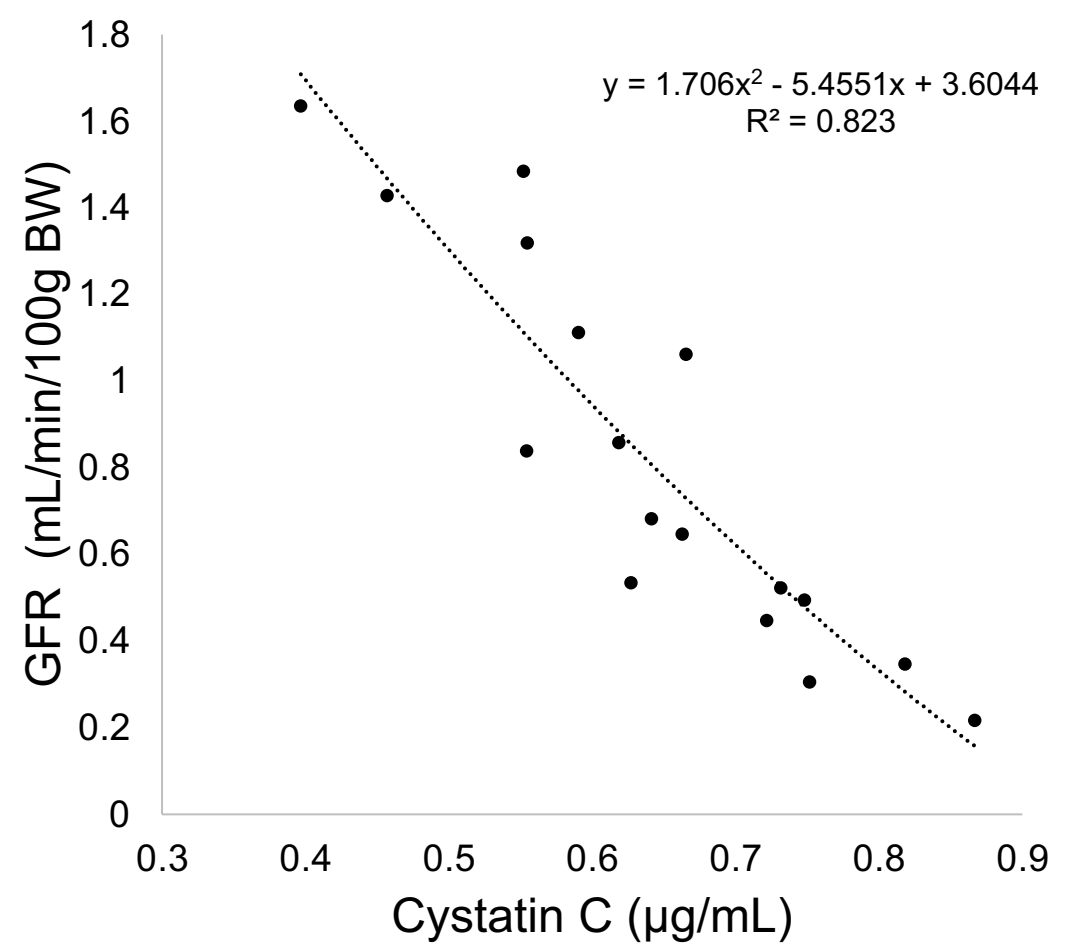
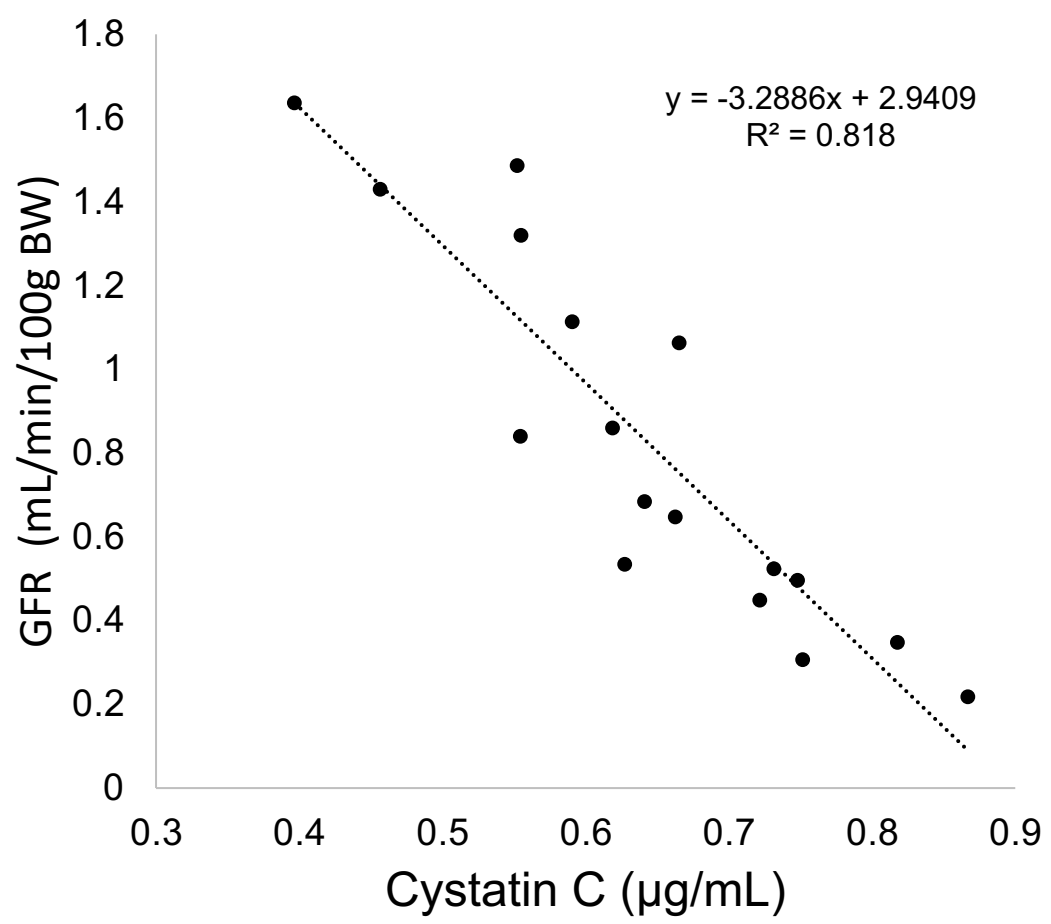
Table S3. MRM Mass Spectrometer Settings, confirmatory quantification by isotope dilutional MS

Positive ion mode				
Metabolite	Parent ion m/z	Daughter ion m/z	Collision energy (V)	Retention Time (min)
Tryptophan	205.2	146	25	4.98
Tryptophan-d5	210	150	25	4.94
Kynurenine	209.2	94	22	4.42
Kynurenine-d4	213.2	98	22	4.39
kynurenic acid	190.2	144	25	5.18
Nicotinamide	123.1	80	25	4.57
nicotinamide-13C6	129.1	85	25	4.59
nicotinamide mononucleotide	335.2	123	20	2.84
Nicotinamide riboside	255.0	123.0	20	3.16
Indole-3-acetic acid	176.1	130.0	25	7.28
Indole-3-propionic acid	190.1	130.0	25	8.18
NAD+	664.4	428.0	25	3.94
NAD+-d5	669.4	428.0	25	3.94
NADH	665.4	524	25	3.30
Curtain gas: 25, GS1 0, GS2 0, Spray voltage 3000V, Source temperature 400°C.				
Declustering potential 75, Entrance potential 5, collision excitation potential 15, collision gas 6.				
Negative ion mode				
Quinolinic acid	166.1	78	-25	2.91
Quinolinic acid-13C3, 15N1	170.1	82	-25	3.03
Indoxyl sulfate	212.2	80	-25	5.54
Curtain gas: 25, GS1 0, GS2 0, Spray voltage -3000V, Source temperature 400°C.				
Declustering potential -75, Entrance potential -5, collision excitation potential -15, collision gas Medium.				

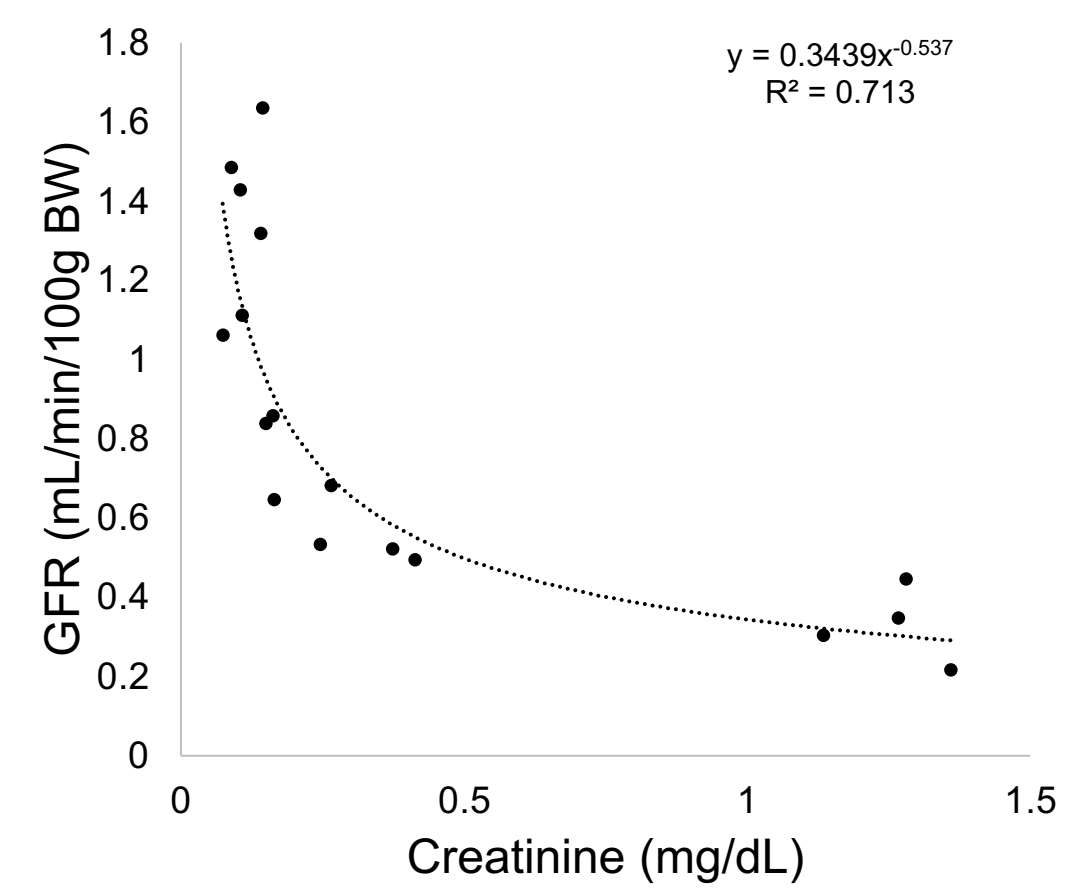
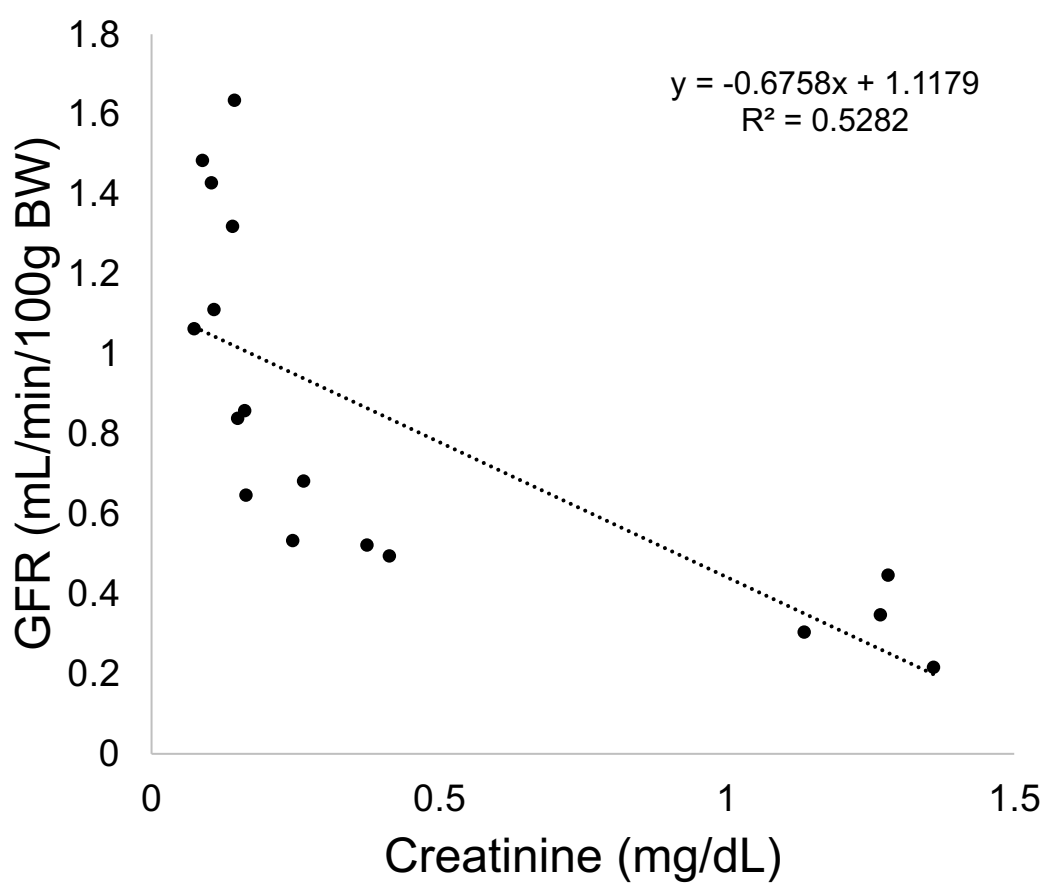
Supplemental Figure 1. Phenotypes of Sham and Uninephrectomized mice during Pregnancy

(A) Correlation of plasma cystatin C levels with directly measured GFR measured as described in Methods (n=17) in mouse models with varying degrees of renal insufficiency. Plasma cystatin C levels showed a strong negative correlation with GFR using both linear ($R^2= 0.82$) and polynomial models ($R^2= 0.82$). **(B)** Correlation of plasma creatinine levels with glomerular filtration rate (GFR) measured as described in Methods (N=17). Plasma creatinine level showed a modest relationship with measured GFR using both linear ($R^2= 0.53$) or power models ($R^2= 0.71$) **(C)** Plasma cystatin C measurements at baseline, Day 1, Day 7 and Day 14 after surgery in control (Sham) and uninephrectomized (UNx) mice. **(D)** Estimated glomerular filtration rate (eGFR) at baseline, Day 1, Day 7 and Day 14 after surgery was calculated in Sham and UNx mice as described in Methods. **(E)** Body weights of Sham and UNx mice throughout pregnancy. **(F)** Gestational day 18 (GD18) left kidney weights in Sham and UNx mice. Data were normalized with body weight values. Data depicted as mean \pm standard deviation. n=6 per group except otherwise indicated. Unpaired 2-tailed *t* test; * $P < 0.05$ in UNx versus Sham mice.

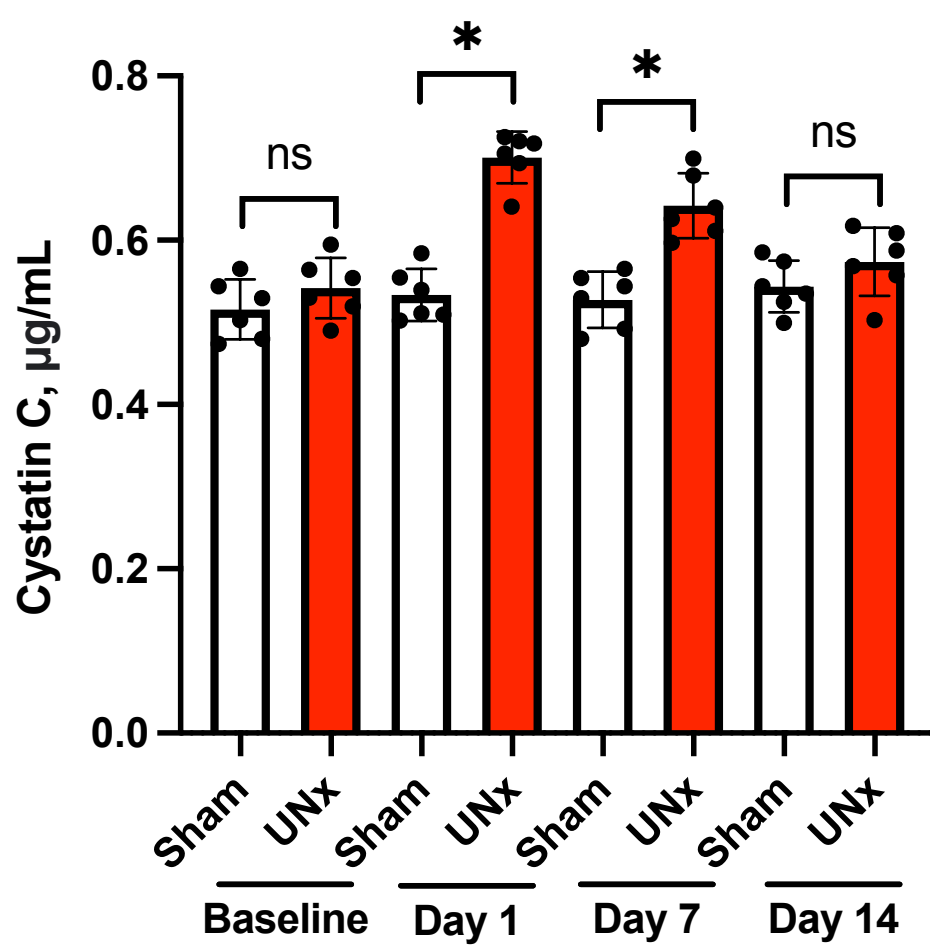
A.



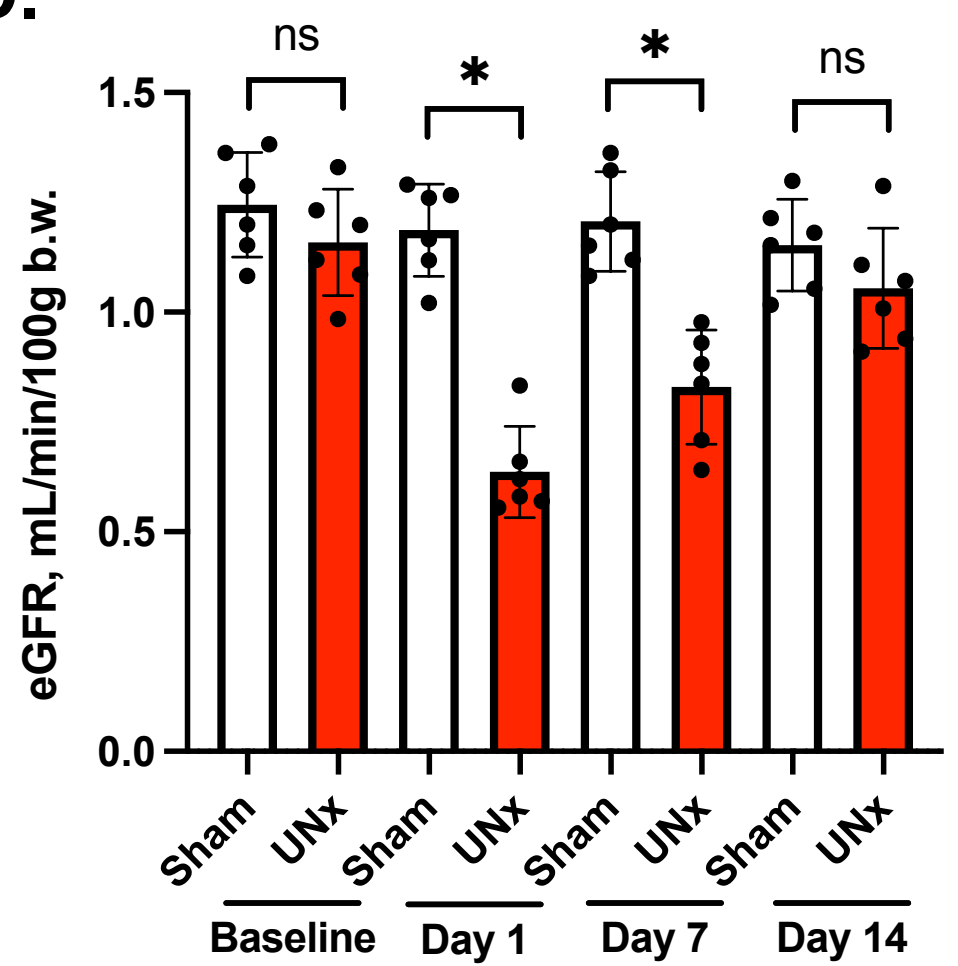
B.



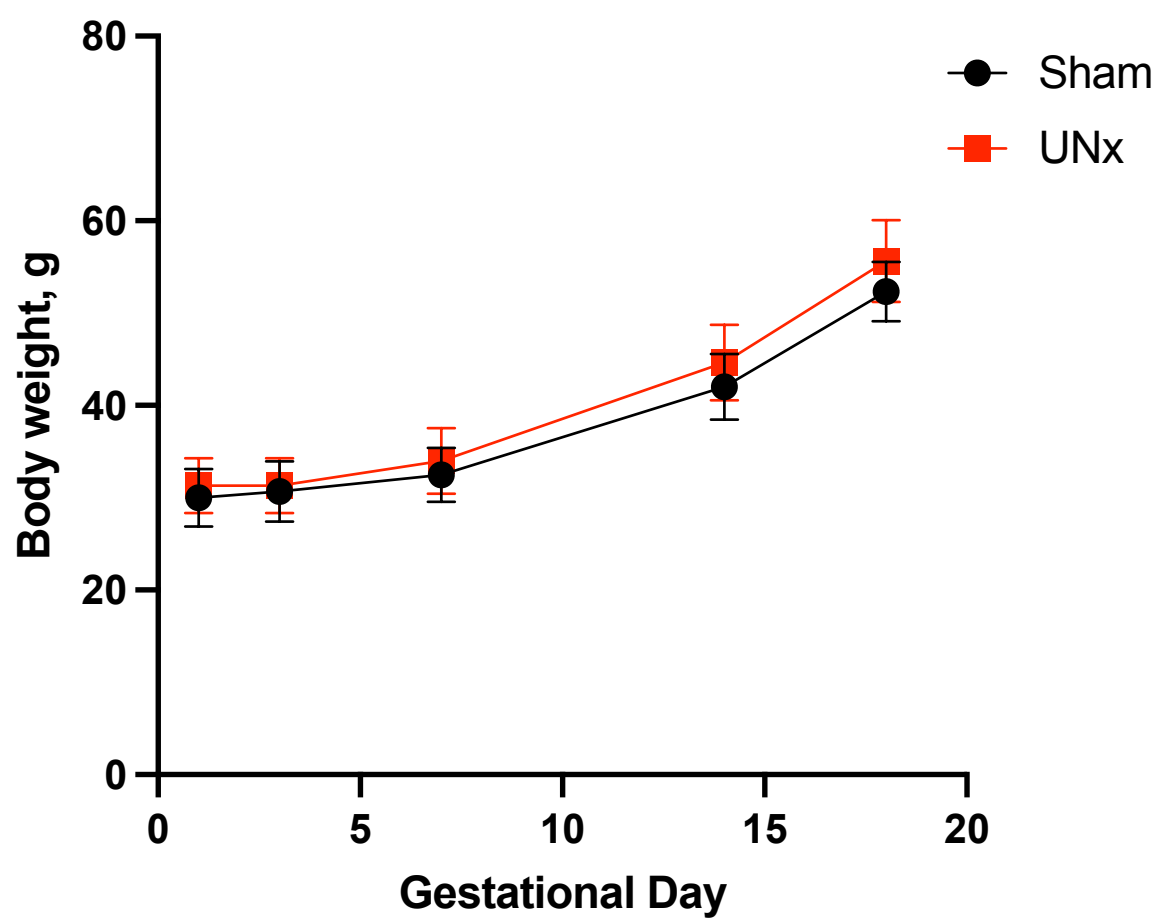
C.



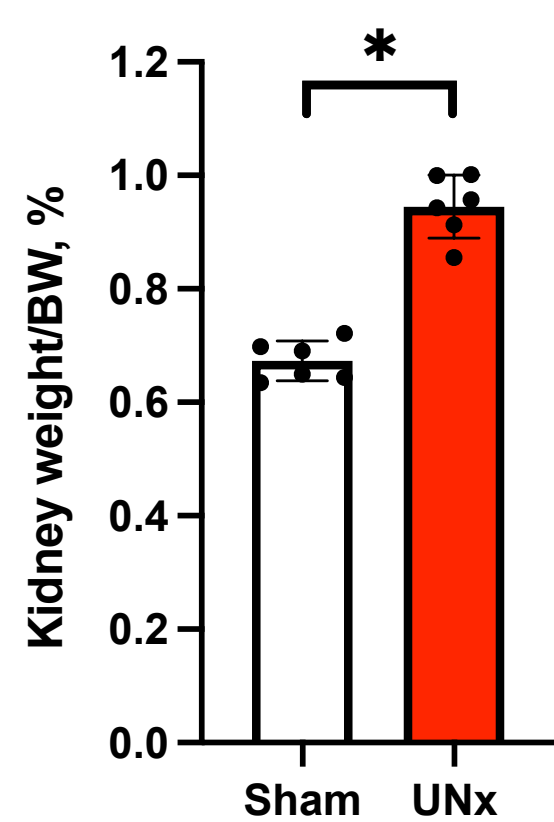
D.



E.

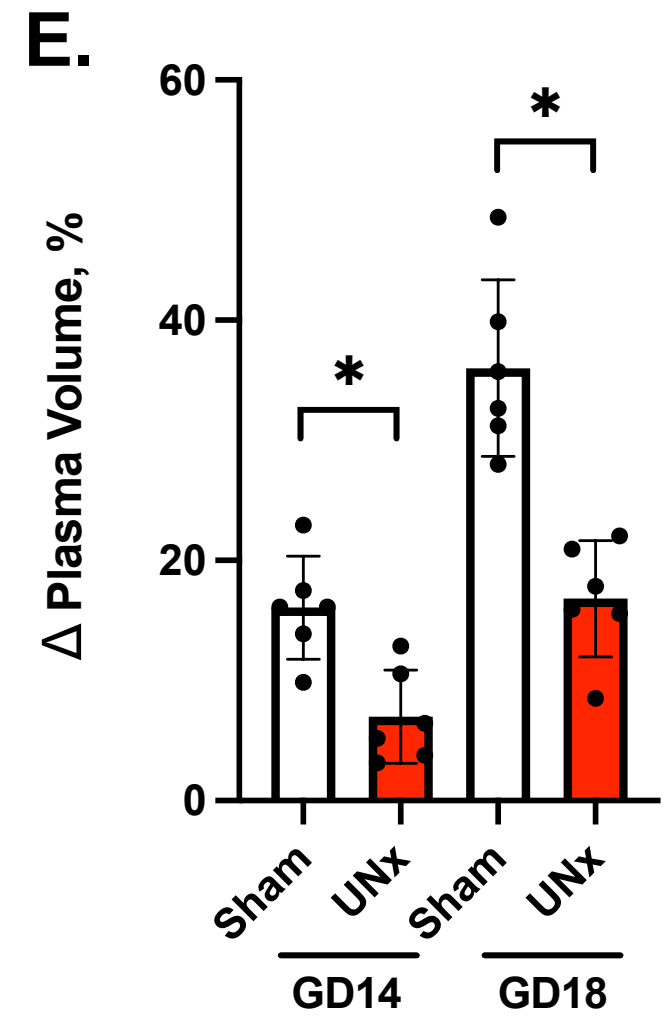
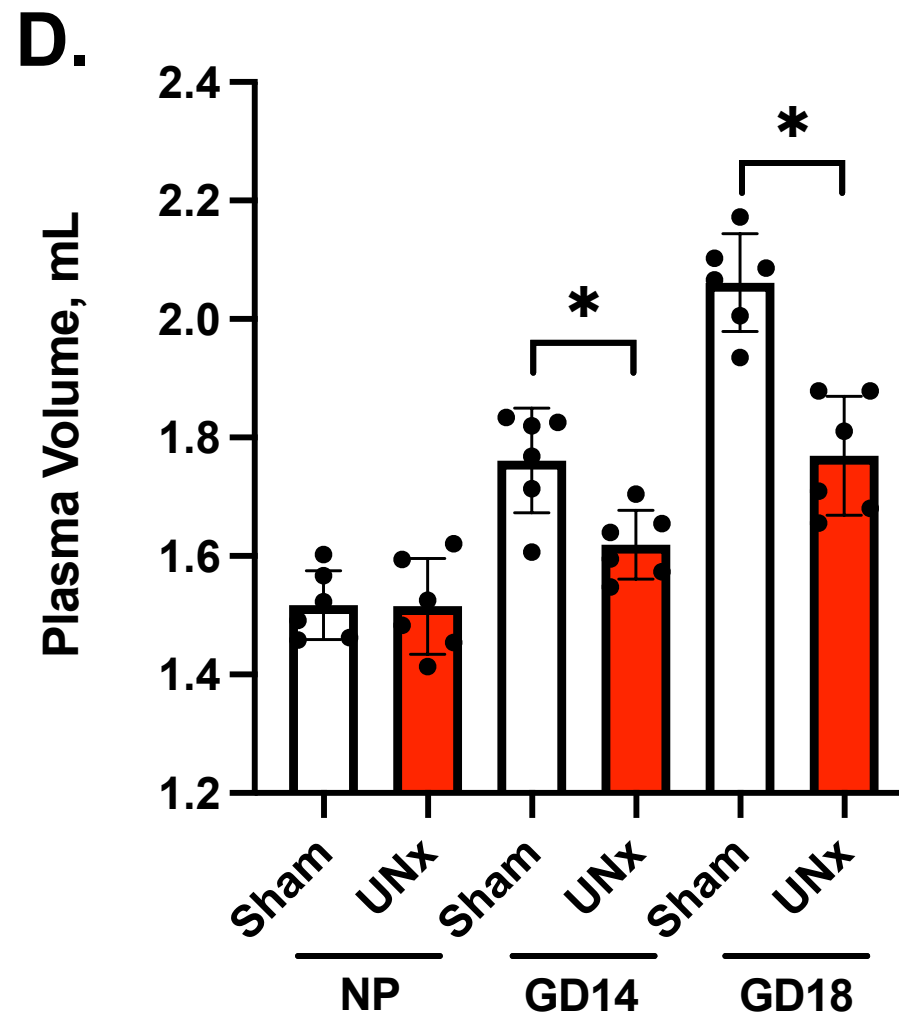
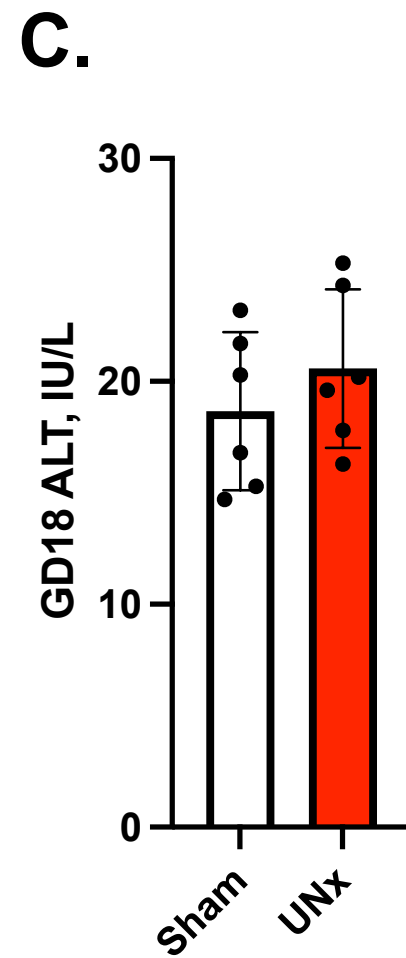
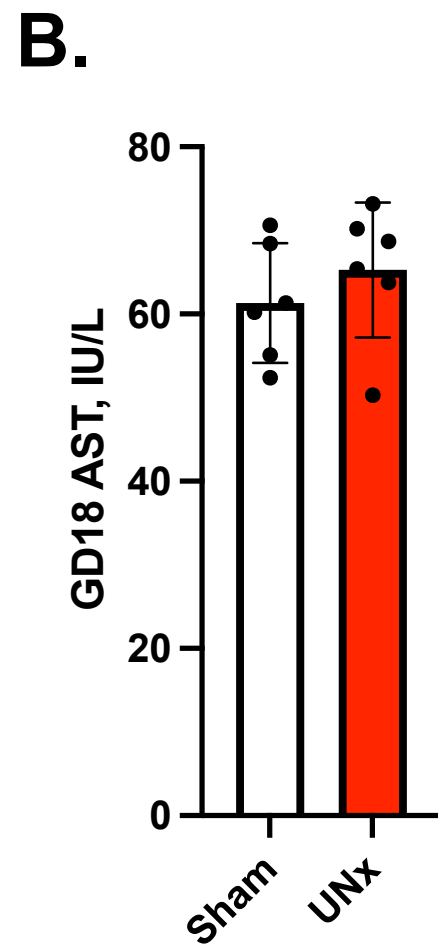
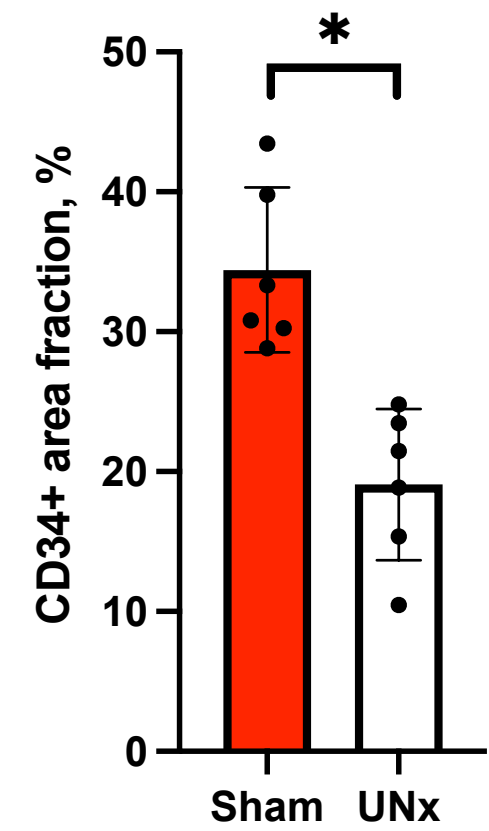
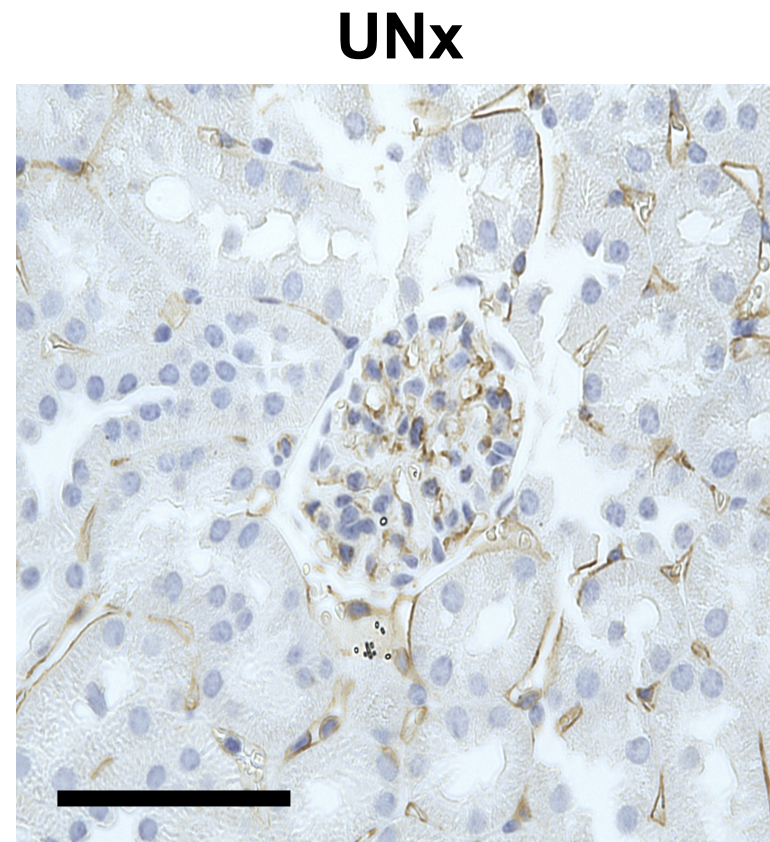
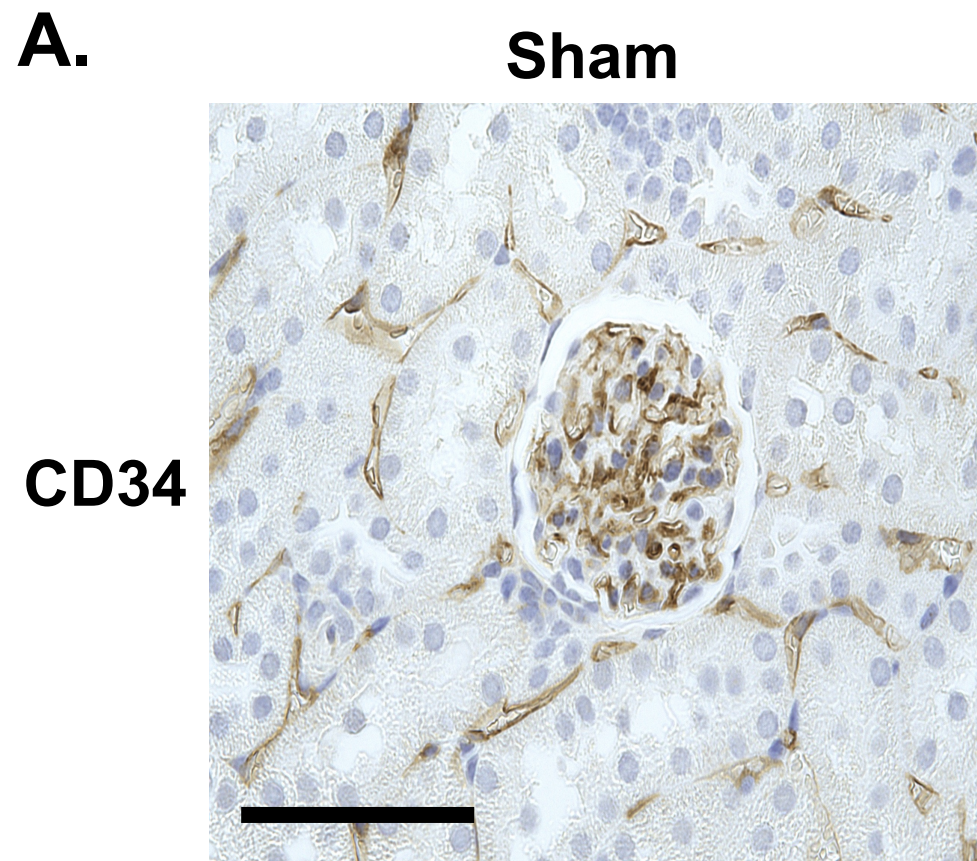


F.



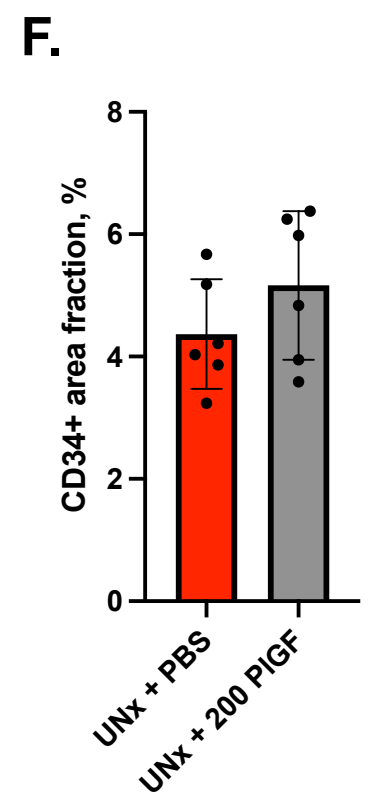
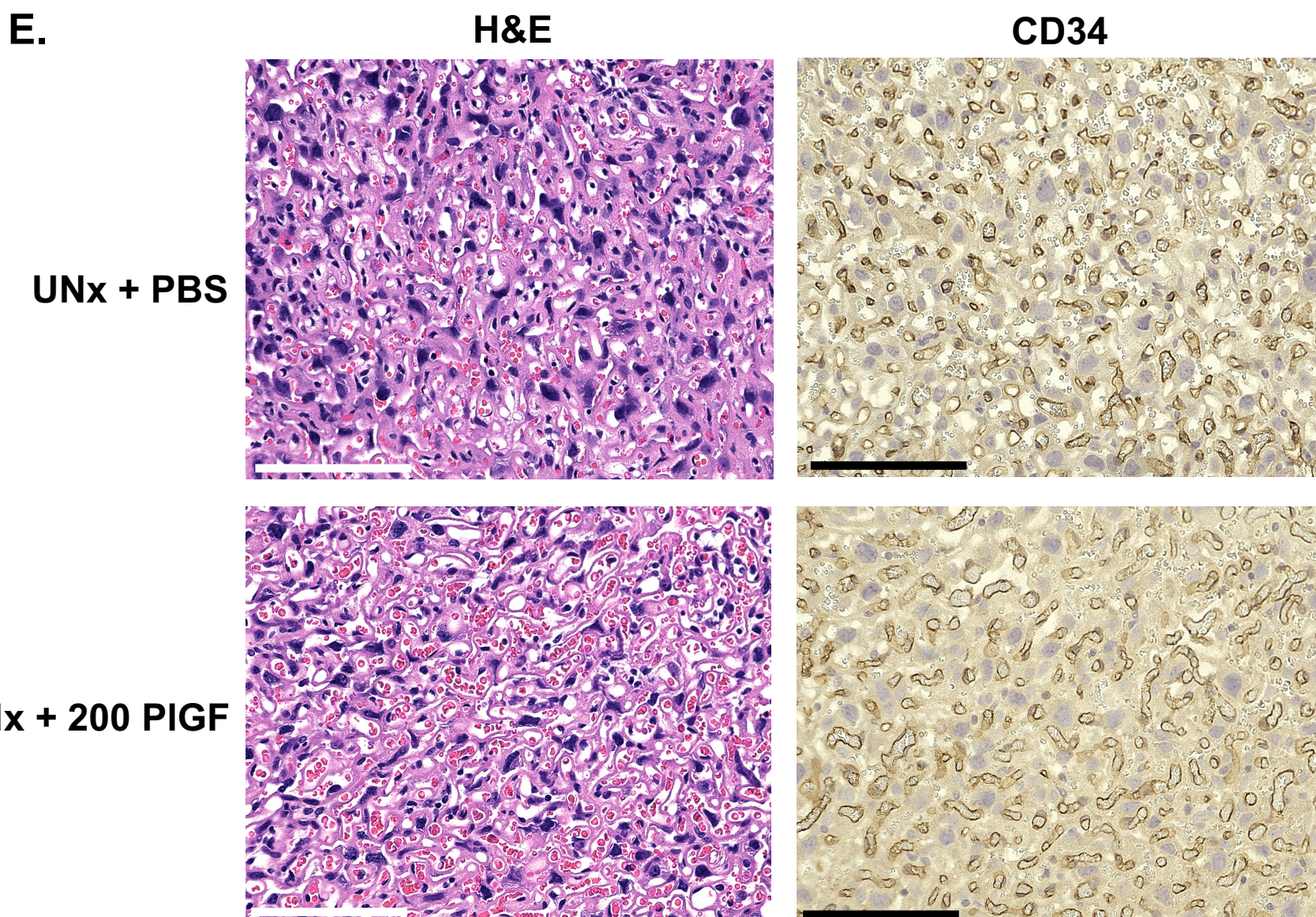
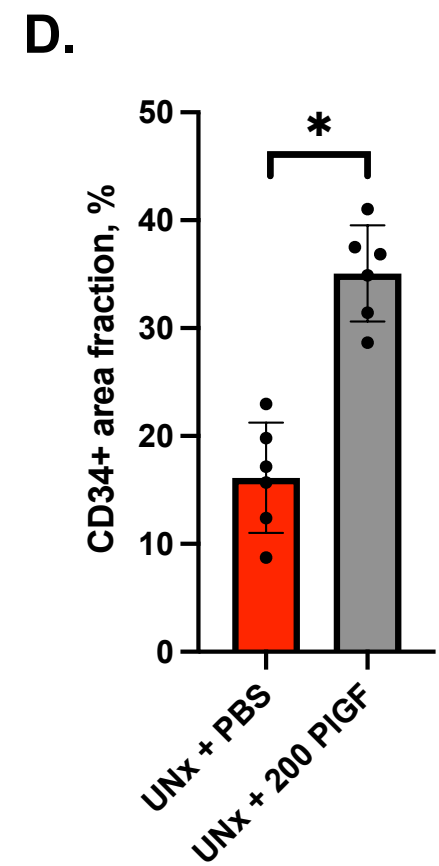
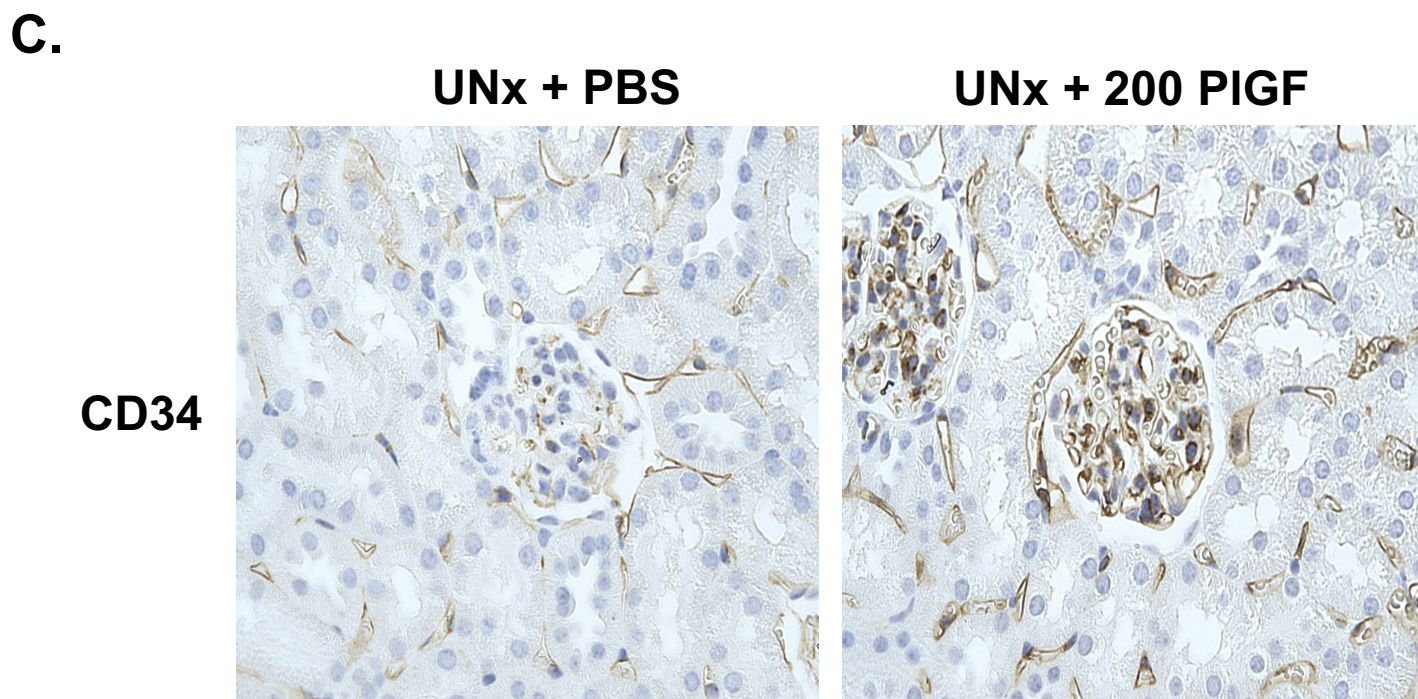
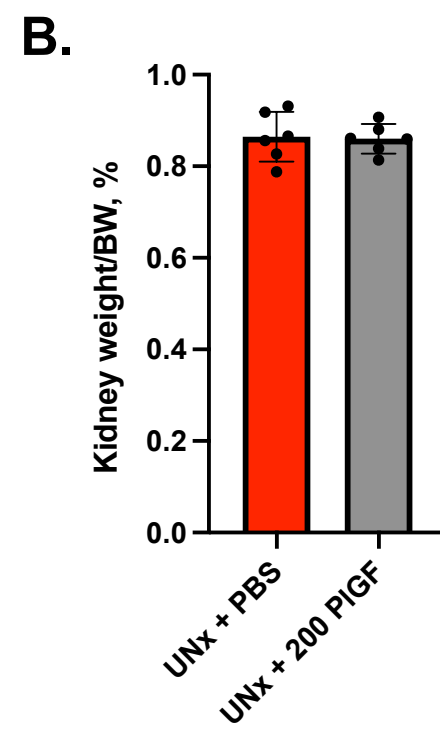
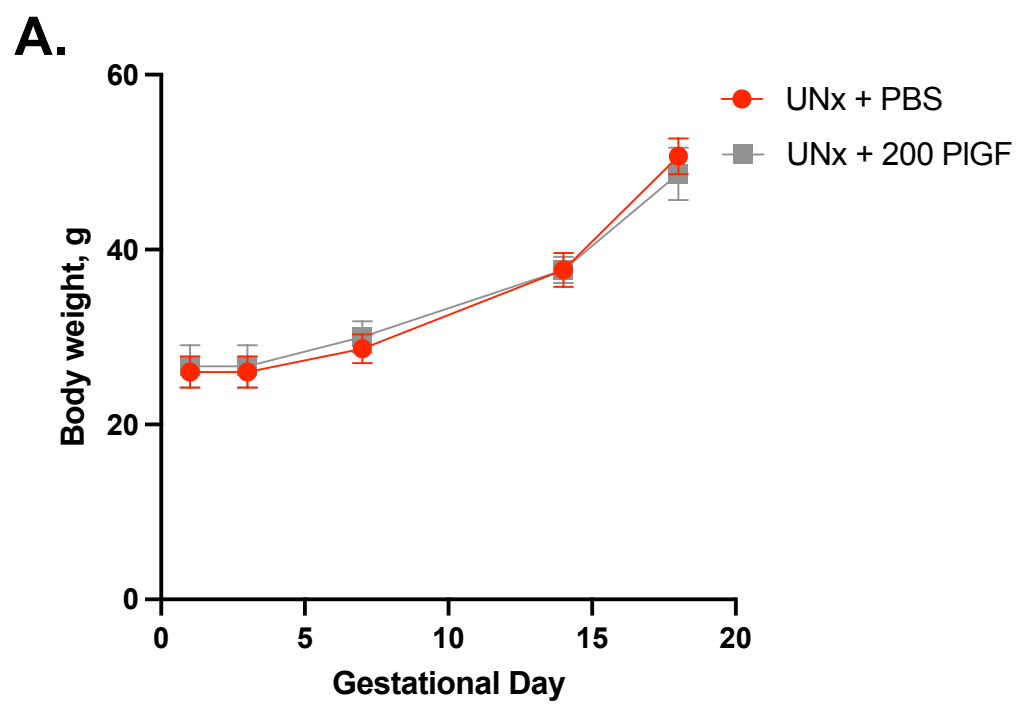
Supplemental Figure 2. Additional Features of the Impact of Prior Uninephrectomy on Pregnancy in mice

(A) CD34 immunohistochemistry analysis of renal tissue at GD18 from one representative control (Sham, left panel) and one uninephrectomized (UNx, right panel) mice. UNx mice exhibit loss of CD34 positive endothelial cells among glomerular capillaries (scale bar=125 μ m). Summary data for the CD34 positive glomerular area quantified using ImageJ software in Sham and UNx mice at GD18 is depicted. GD18 plasma aspartate aminotransferase (AST) **(B)** and alanine aminotransferase **(C)** measurements in Sham and UNx mice. **(D)** Plasma volume measurements in Sham and UNx mice in non-pregnant (NP) state, at GD14 and GD18, and shown as change when compared with NP values **(E)**. Data were normalized with body weight values. Data depicted as mean \pm standard deviation. n=6 per group except otherwise indicated. Unpaired 2-tailed *t* test; **P* < 0.05 in UNx versus Sham mice.



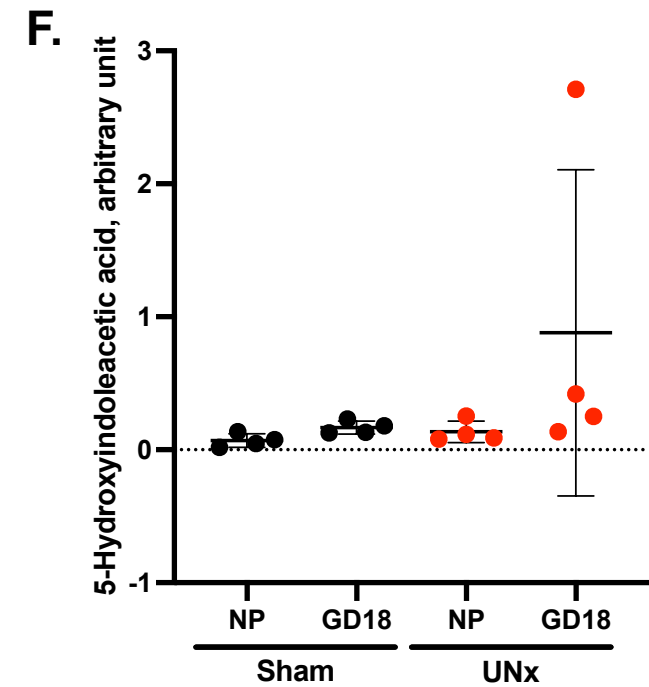
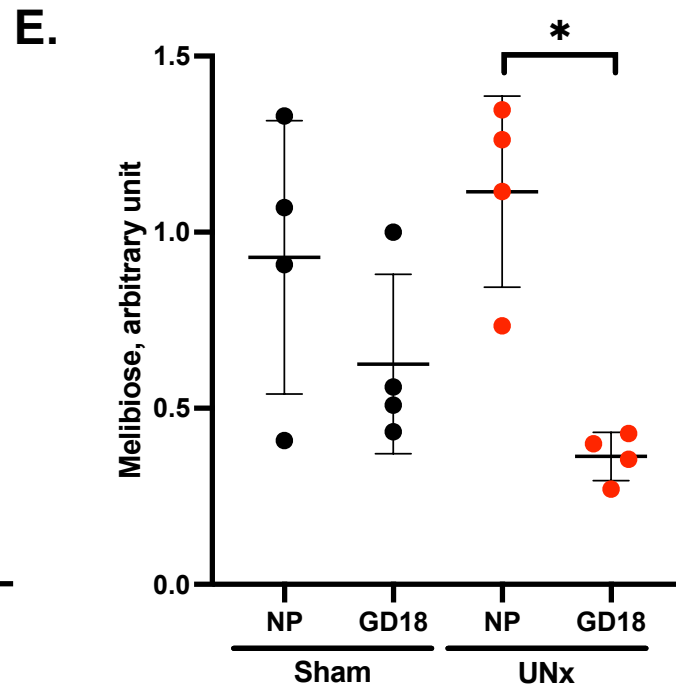
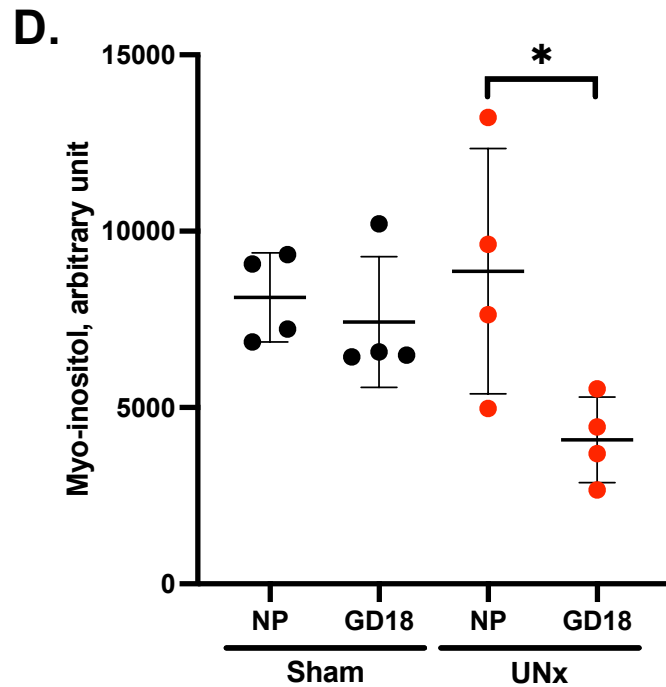
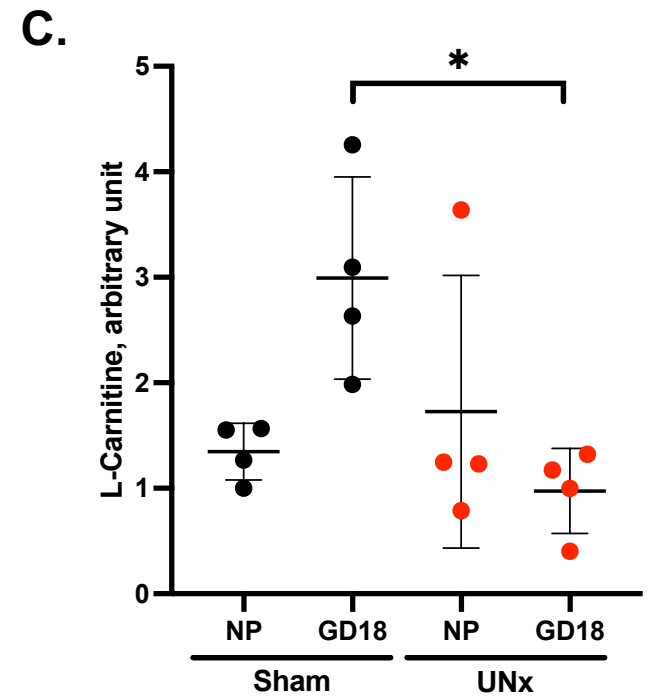
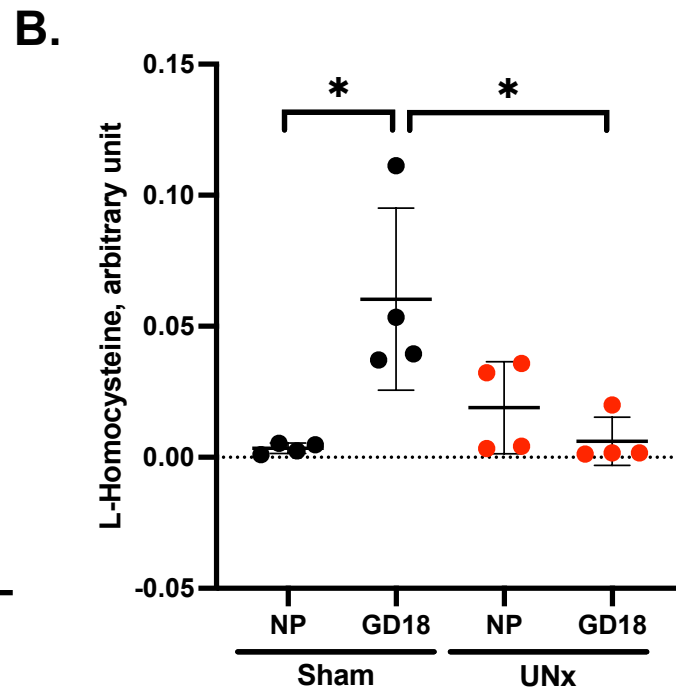
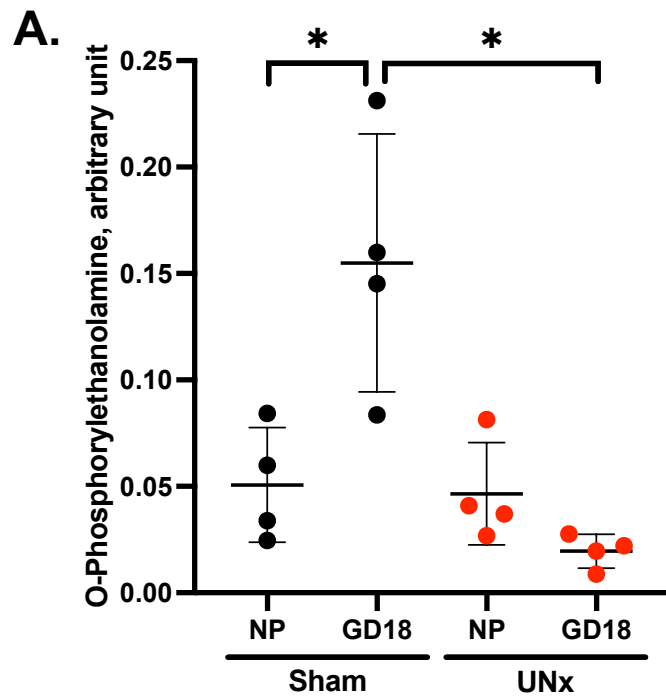
Supplemental Figure 3. Phenotypes of Uninephrectomized mice treated with PBS or Placental Growth Factor

(A) Body weights of uninephrectomized (UNx) mice treated with either PBS or placental growth factor (PIGF) throughout pregnancy. **(B)** Gestational day 18 (GD18) left kidney weights in UNx mice treated with PBS or PIGF. Data were normalized with body weight values. **(C)** CD34 immunohistochemistry analysis of renal tissue at GD18 from one representative UNx mice treated with PBS (left panel) or PIGF (right panel). PIGF treatment increased CD34 positive area among glomeruli in late pregnant UNx mice (scale bar= 125 μ m). **(D)** Summary data for the CD34 positive glomerular area quantified using ImageJ software in UNx mice treated with PBS or PIGF at GD18 is depicted. **(E)** Histopathological analysis of placenta tissue from one representative UNx mice treated with PBS (upper panel) or PIGF (lower panel) at GD18 (scale bar= 125 μ m). H&E stain and CD34 stain shows similar labyrinthine vasculature in UNx mice treated with PBS or PIGF. **(F)** Summary data for the CD34 immunohistochemistry quantitated within the labyrinth (using ImageJ software) between UNx mice treated with PBS or PIGF. Data depicted as mean \pm standard deviation. n=6 per group. Unpaired 2-tailed *t* test; **P* < 0.05 in in UNx mice treated with PIGF versus PBS.



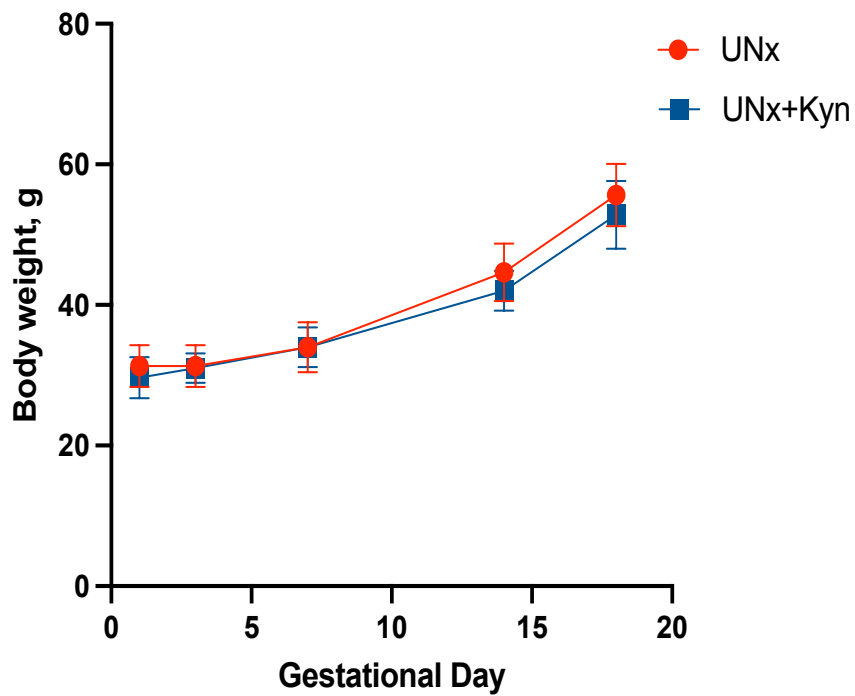
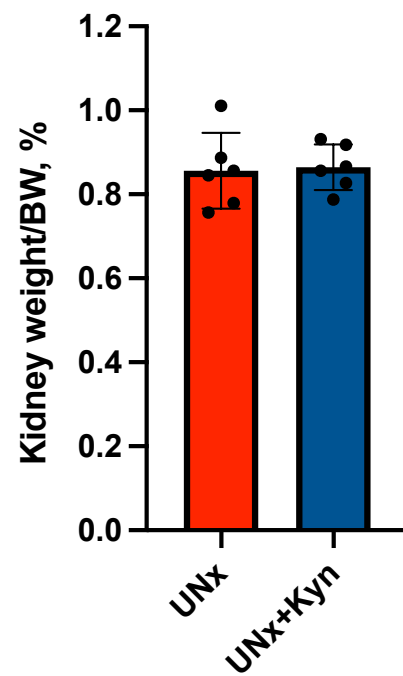
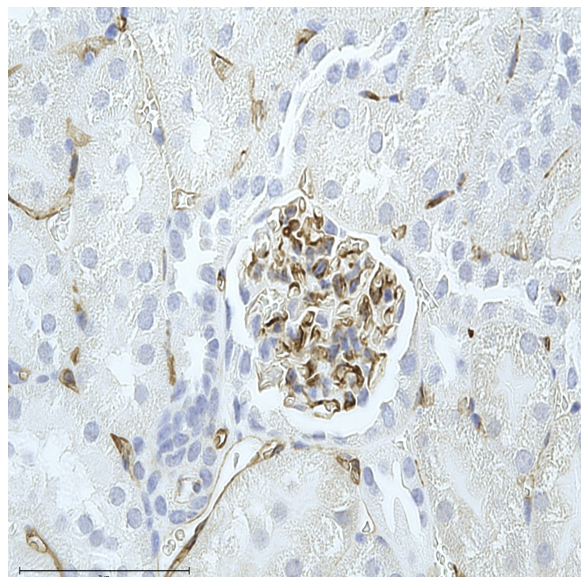
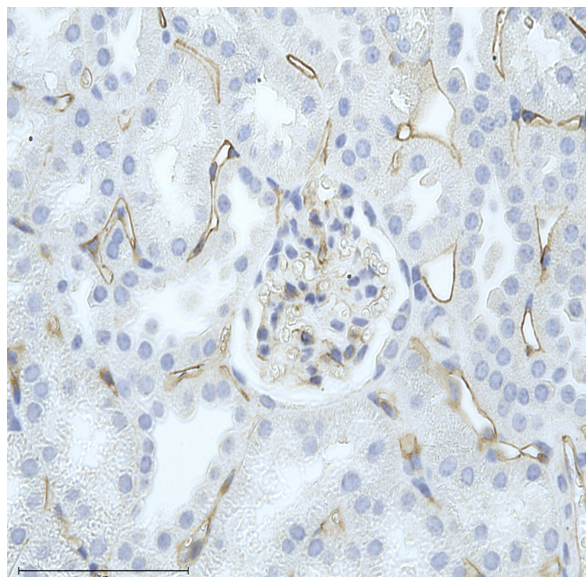
Supplemental Figure 4. Trends in Metabolites Levels during Pregnancy in Sham and Uninephrectomized Mice from Metabolite platform

Levels of O-phosphorylethanolamine **(A)**, L-homocysteine **(B)**, L-carnitine **(C)**, Myo-inositol **(D)**, Melibiose **(E)** and 5-Hydroxyindoleacetic acid **(F)** on the metabolite platform in non-pregnant (NP) state and at gestational day 18 (GD18) in Sham and uninephrectomized (UNx) mice. Results shown are normalized peak intensities (arbitrary unit) as individual values and as mean \pm standard deviations for each of the metabolites. n=4 per group. 1-way ANOVA with Tukey's test for multiple comparisons; * $P < 0.05$.



Supplemental Figure 5. Phenotypes of Uninephrectomized mice treated with L-Kynurenine versus Uninephrectomized Mice during Pregnancy

(A) Body weights of uninephrectomized (UNx) mice and UNx mice treated with L-kynurenine 25mg/L added to drinking water (UNx+Kyn) throughout pregnancy. **(B)** Gestational day 18 (GD18) left kidney weights in UNx and UNx+Kyn mice. Data were normalized with body weight values. **(C)** CD34 immunohistochemistry analysis of renal tissue at GD18 from one representative UNx (left panel) and one UNx+Kyn mice (right panel). L-kynurenine supplementation increased CD34 positive area among glomeruli in late pregnant UNx mice (scale bar= 125 μ m). **(D)** Summary data for the CD34 positive glomerular area quantified using ImageJ software in UNx and UNx+Kyn mice at GD18 is depicted. Data represent the mean \pm standard deviation. n=6 per group. Unpaired 2-tailed *t* test; **P* < 0.05 in UNx+Kyn versus UNx mice.

A.**B.****C.****UNx****UNx+Kyn****D.**